

Article

Reversible Thiol Oxidation Increases Mitochondrial Electron Transport Complex Enzyme Activity but Not Respiration in Cardiomyocytes from Patients with End-Stage Heart Failure

Ravi A. Kumar ¹, Trace Thome ¹, Omar M. Sharaf ², Terence E. Ryan ¹, George J. Arnaoutakis ³, Eric I. Jeng ^{3,†} and Leonardo F. Ferreira ^{1,4,*,†}

¹ Department of Applied Physiology and Kinesiology, University of Florida, Gainesville, FL 32611, USA; rakumar@ufl.edu (R.A.K.); trthome@ufl.edu (T.T.); ryant@ufl.edu (T.E.R.)

² College of Medicine, University of Florida, Gainesville, FL 32611, USA; omar.sharaf@ufl.edu

³ Department of Surgery, Division of Thoracic and Cardiovascular Surgery, University of Florida, Gainesville, FL 32611, USA; george.arnaoutakis@surgery.ufl.edu (G.J.A.); eric.jeng@surgery.ufl.edu (E.I.J.)

⁴ Department of Physiology, Amsterdam UMC, 1081 HZ Amsterdam, The Netherlands

* Correspondence: ferreira@hhp.ufl.edu; Tel.: +1-352-294-1724

† These authors contributed equally to this work.

Abstract: Cardiomyocyte dysfunction in patients with end-stage heart failure with reduced ejection fraction (HFrEF) stems from mitochondrial dysfunction, which contributes to an energetic crisis. Mitochondrial dysfunction reportedly relates to increased markers of oxidative stress, but the impact of reversible thiol oxidation on myocardial mitochondrial function in patients with HFrEF has not been investigated. In the present study, we assessed mitochondrial function in ventricular biopsies from patients with end-stage HFrEF in the presence and absence of the thiol-reducing agent dithiothreitol (DTT). Isolated mitochondria exposed to DTT had increased enzyme activity of complexes I ($p = 0.009$) and III ($p = 0.018$) of the electron transport system, while complexes II ($p = 0.630$) and IV ($p = 0.926$) showed no changes. However, increased enzyme activity did not carry over to measurements of mitochondrial respiration in permeabilized bundles. Oxidative phosphorylation conductance ($p = 0.439$), maximal respiration ($p = 0.312$), and ADP sensitivity ($p = 0.514$) were unchanged by 5 mM DTT treatment. These results indicate that mitochondrial function can be modulated through reversible thiol oxidation, but other components of mitochondrial energy transfer are rate limiting in end-stage HFrEF. Optimal therapies to normalize cardiac mitochondrial respiration in patients with end-stage HFrEF may benefit from interventions to reverse thiol oxidation, which limits complex I and III activities.

Keywords: redox; mitochondria; cardiac; heart failure; HFrEF; bioenergetics



Citation: Kumar, R.A.; Thome, T.; Sharaf, O.M.; Ryan, T.E.; Arnaoutakis, G.J.; Jeng, E.I.; Ferreira, L.F. Reversible Thiol Oxidation Increases Mitochondrial Electron Transport Complex Enzyme Activity but Not Respiration in Cardiomyocytes from Patients with End-Stage Heart Failure. *Cells* **2022**, *11*, 2292. <https://doi.org/10.3390/cells11152292>

Academic Editors: Michael Reid, Li Li Ji and Scott Powers

Received: 30 May 2022

Accepted: 21 July 2022

Published: 25 July 2022

Publisher's Note: MDPI stays neutral with regard to jurisdictional claims in published maps and institutional affiliations.



Copyright: © 2022 by the authors. Licensee MDPI, Basel, Switzerland. This article is an open access article distributed under the terms and conditions of the Creative Commons Attribution (CC BY) license (<https://creativecommons.org/licenses/by/4.0/>).

1. Introduction

Heart failure with reduced ejection fraction (HFrEF) describes the inability of the heart to adequately pump blood due to impaired systolic function. End-stage HFrEF refers to a diagnostic category in which patients are non-responsive to conventional treatments and instead require advanced therapies, such as heart transplantation or the placement of a mechanical pump to assist the heart (left ventricular assist device; LVAD). Insufficient ventricular function in HFrEF stems from contractile and energetic deficiencies. Mitochondria provide ~90% of ATP for continuously contracting cardiomyocytes, and myocardial mitochondrial function decreases with HFrEF [1–5]. Inadequate mitochondrial function leads to energy depletion, which contributes to contractile dysfunction, and correlates with disease severity [6] and patient mortality [7,8]. As such, targeting the mitochondria has gained increasing attention as an approach to improve myocardial function and disease outcomes in patients with HFrEF, especially for those that are not responsive to conventional pharmaceutical therapies [9–11].

One contributing factor to mitochondrial dysfunction is the accumulation of reactive oxygen species (ROS), which results in the excessive oxidation of proteins, lipids, and DNA. Cysteine residues are favorable targets for reversible redox reactions because of their thiol moiety (R-SH). Cysteine oxidation is a characteristic feature of normal cell signaling; however, excessive oxidation can alter protein structure and function [12,13]. Mitochondria are considered a major source of increased oxidants in the failing heart and, by proximity, are also a primary target for redox reactions [12,13]. Redox proteomics in left ventricle biopsies from patients with end-stage HFrEF reveal increases in reversibly oxidized cysteine residues in proteins of complexes I and II of the electron transport system (ETS) in cardiac mitochondria [14]. The reversible oxidation of thiol moieties causes mitochondrial dysfunction in cardiomyocytes from mice fed a high-fat, high-sucrose diet [15] and those from rats treated with doxorubicin [16]. Therefore, the mitochondrial limitations in patients with end-stage HFrEF may be caused by the oxidative modifications of thiol redox switches, such as those found in complexes I and II [14], which impair mitochondrial protein function.

The objective of this study was to determine if an acute reduction of reversibly oxidized thiol moieties with dithiothreitol (DTT) could increase mitochondrial ETS complex activity and respiration at several levels of energetic demand in left ventricular biopsies from patients with end-stage HFrEF.

2. Materials and Methods

2.1. Human Subjects

All experiments involving human subjects received approval by the Institutional Review Board of the University of Florida (protocol #202000853). Patients were informed of the nature and purpose of the study, and they signed a written consent in accordance with the Declaration of Helsinki. Patients with heart failure with reduced ejection fraction (HFrEF) undergoing the placement of a left ventricular assist device (LVAD) were recruited to participate in this study. Our inclusion criteria included subjects 18 years or older with end-stage HFrEF for more than one year. Patients with both ischemic and non-ischemic HFrEF were recruited. Patients were excluded from consideration if they presented with severe lung, hepatic, or renal disease, or treatment with cancer chemotherapy. Echocardiography was performed on the morning of the procedure as part of clinical care, and the results are reported here for patient characterization.

2.2. Biopsy Collection

Surgeries and biopsy collections were performed by cardiothoracic surgeons. As part of the LVAD placement, a portion of the left ventricle apical core was removed to insert the device. Apical core biopsies were immediately placed in ice-cold Buffer X (in mM: 7.23 K₂EGTA, 2.77 Ca-K₂EGTA, 20 imidazole, 20 taurine, 5.7 ATP, 14.3 PCr, 6.56 MgCl₂-6H₂O, 50 K-MES; pH 7.1). We rinsed and dissected myocardial tissue that was visibly free from fat, scarring, fibrosis, and connective tissue, and immediately began prepping a portion of the sample for the measurement of mitochondrial respiration. The remaining myocardial tissue was quickly flash frozen in liquid nitrogen for the later isolation of mitochondria and measurement of ETS complex activity.

2.3. Preparation of Permeabilized Cardiomyocyte Bundles and Mitochondrial Respiration

Fine-tipped tweezers were used to separate cardiomyocyte bundles along the longitudinal axis to expose maximal cardiomyocyte surface area. We permeabilized ~2–4 mg (wet weight; WW) bundles in Buffer X containing saponin (30 µg/mL) for 30 min while gently rotating at 4 °C. Bundles were then washed 3 × 5 min in Buffer D (in mM: 30 KCl, 10 KH₂PO₄, 5 MgCl₂-6H₂O, 105 K-MES, and 2.5 mg/mL BSA, 1 EGTA, pH 7.1). In bundles treated with DTT, a series of washes was carried out in the presence of 5 mM DTT in Buffer D. We chose this concentration based on a previous study [15]. We then proceeded with measurements of mitochondrial respiration.

We performed high-resolution O_2 respirometry at 37 °C in Buffer D supplemented with 5 mM creatine monohydrate and 10 μ M blebbistatin using an O2K Oxygraph (Oroboros, Innsbruck, Austria). To provide a comprehensive and physiologically relevant assessment of mitochondrial respiration, we implemented the previously described creatine kinase clamp, which permits control over the extramitochondrial energy demand (ADP/ATP) [17,18]. Mitochondrial respiration has traditionally been measured under saturating conditions of ADP, which override the mitochondrial internal mechanism of responding to energetic demand, whereas this approach permits the assessment of mitochondrial oxygen consumption (JO_2) at varying levels of energetic demand (ΔG_{ATP}), which correspond to physiologically relevant levels of cellular ATPase activity. State 2 respiration was initiated by the addition of 10 mM pyruvate and 2 mM malate. The creatine kinase clamp was then established by the addition of 20 U/mL creatine kinase, 5 mM Tris-ATP, and 1 mM phosphocreatine (PCr). These conditions (1 mM PCr) model near-maximal mitochondrial energetic demand *in vitro*. We then added 10 mM Cytochrome C to assess mitochondrial membrane integrity. Extramitochondrial energetic demand was then decreased by additional titrations of PCr (1–30 mM) to experimentally set different ATP free-energy states through adjustments to the Cr/PCr ratio. The rate of oxygen consumption (JO_2 in pmol/s) was calculated under each of these conditions and plotted against ΔG_{ATP} to establish a linear ‘force–flow’ relationship, where the slope represents the conductance of the ETS. Conductance measures the ability of mitochondria to respond to varying levels of energetic demand, akin to an exercise stress test. All measurements were conducted within an O_2 range of ~200 to 350 μ M. Bundles were excluded from analysis if the addition of Cytochrome C resulted in a 15% increase in respiration, indicating mitochondrial outer-membrane damage during preparation. Following experiments, bundles were collected and freeze-dried using a bench-top freeze-dry system (Labconco, Kansas City, MO, USA), and the results were normalized by bundle dry weight (DW) (JO_2 -pmol/s/mg DW). Where feasible, samples were run in duplicate, and the results were averaged together.

We additionally calculated the corresponding ADP concentrations at each energetic state using the bioenergetics calculator provided by Fisher-Welman et al. [18]. These concentrations were used to determine mitochondrial ADP kinetics using the Michaelis–Menten equation to calculate maximal respiration (JO_{2Max} or V_{max}) and the Michaelis constant (ADP₅₀ or K_m).

2.4. Mitochondrial Isolation

Mitochondria were isolated from previously frozen myocardial tissue using the methods described by Thome et al. [19] with slight adaptation. Samples (~100–200 mg) were first incubated in PBS containing 10 mM EDTA and 3 mg/mL Collagenase Type I at 37 °C for 30 min to dissociate connective tissue in the especially fibrous human heart samples. All subsequent steps were performed on ice or at 4 °C. Samples were minced for 5 min, and homogenates were transferred to PBS with 10 mM EDTA and 0.5 mg/mL trypsin for an additional 5 min digestion. Next, we centrifuged samples at 500 \times g for 5 min, poured off the supernatant, and resuspended the pellet in mitochondrial isolation medium (MIM; in mM: 50 MOPS, 100 KCl, 1 EGTA, 5 MgSO₄) with 2 mg/mL fatty-acid-free BSA. Samples were then homogenized using a glass–Teflon homogenizer (Wheaton) (6 passes at 40 rpm) and centrifuged at 800 \times g to pellet nonmitochondrial myofibrillar proteins, nuclei, and other cellular components. The supernatant was collected and centrifuged at 10,000 \times g for 10 min to pellet mitochondria, which were then gently resuspended in a small volume of MIM without BSA. We determined the protein concentration of the resuspension using the DC Assay (BioRad) and diluted all samples to 2 mg/mL with MIM.

2.5. Mitochondrial Complex Activity Assays

Mitochondrial complex activities were determined spectrophotometrically from isolated mitochondria using previously described methods [19,20]. Isolated mitochondria were diluted 1:1 in either hypotonic buffer (in mM: 25 K₂HPO₄, 5.3 MgCl, pH 7.2) for

complexes I and IV or Cell Lytic M (Millipore-Sigma; Burlington, NJ, USA) for complexes II and III. Samples prepared in hypotonic buffer were subjected to four freeze–thaw cycles to optimize enzyme activity. All assays were run in duplicate under control conditions or in the presence of 5 mM DTT in a 96-well plate, and changes in absorbance were tracked using a microplate reader (Synergy 2, BioTek/Agilent, Santa Clara, CA, USA). This concentration was selected based on similar experiments in a previous study [15]. Background activities for each assay under control and DTT conditions were calculated during simultaneous reactions using inhibitors specific for each complex. Enzyme activity was calculated as the rate of change in absorbance after background subtraction.

Complex I (NADH: ubiquinone oxidoreductase) activity was measured in 10 mM KH_2PO_4 and 40 mM K_2HPO_4 (pH 7.5) with 3 mg/mL BSA, 240 μM KCN, 4 μM antimycin A, 50 μM decyl-ubiquinone (DCU), and 80 μM 2,6-dichlorophenolindophenol (DCPIP) using 20 μg of mitochondria. We initiated the reaction with the addition of 1 mM NADH and monitored the reduction of DCPIP at 600 nm. Background activity assays were run in the presence of 25 μM rotenone. Changes in absorbance were monitored over 300 s, and slopes were calculated between 100 and 200 s. Rates were converted to moles using the extinction coefficient $19,100 \text{ M}^{-1} \text{ cm}^{-1}$ for DCPIP absorbance at 600 nm.

Complex II (succinate dehydrogenase; SDH) activity was measured in 10 mM KH_2PO_4 , 2 mM EDTA, and 1 mg/mL BSA (pH 7.8) supplemented with 4 μM rotenone, 0.2 mM Tris-ATP, 10 mM succinate, and 80 μM DCPIP using 5 μg of mitochondria. We initiated the reaction with the addition of 0.08 mM DCU and monitored the reduction of DCPIP at 600 nm. Background activity assays were run in the presence of 10 mM malonate. Changes in absorbance were monitored over 1200 s, and slopes were calculated between 100 and 300 s for DTT-treated samples or between 600 and 800 s for control samples. Rates were converted to moles using the extinction coefficient $19,100 \text{ M}^{-1} \text{ cm}^{-1}$ for DCPIP absorbance at 600 nm.

Complex III (Q-Cytochrome C oxidoreductase) activity was measured in 10 mM KH_2PO_4 , 2 mM EDTA, and 1 mg/mL BSA (pH 7.8) supplemented with 0.2 mM Tris-ATP, 240 μM KCN, and 110 μM oxidized Cytochrome C using 15 μg of mitochondria. We initiated the reaction with the addition of 0.15 mM reduced decyl-ubiquinol (reduced) and monitored the reduction of Cytochrome C at 550 nm. Background activity assays were run in the presence of 10 μM myxothiazol. Changes in absorbance were monitored over 60 s, and slopes were calculated between 15 and 45 s. Rates were converted to moles using the extinction coefficient $18,500 \text{ M}^{-1} \text{ cm}^{-1}$ for Cytochrome C absorbance at 550 nm.

Complex IV (Cytochrome C Oxidase) activity was measured in 10 mM KH_2PO_4 , 250 mM sucrose, and 1 mg/mL BSA (pH 6.5) supplemented with 2.5 mM maltoside and 5 μM antimycin A using 5 μg of mitochondria. We initiated the reaction with the addition of 110 μM reduced Cytochrome C and monitored the oxidation of Cytochrome C at 550 nm. Background activity assays were run in the presence of 0.24 mM KCN. Changes in absorbance were monitored over 300 s, and slopes were calculated between 120 and 180 s. Rates were converted to moles using the extinction coefficient $18,500 \text{ M}^{-1} \text{ cm}^{-1}$ for Cytochrome C absorbance at 550 nm.

2.6. Statistics

Data in the text and tables are presented as mean \pm SD. Individual data (scatterplots) and group means (bars) are shown in figures unless stated otherwise. We performed tests for normality (Shapiro–Wilk) before running paired *t*- (parametric) and Wilcoxon signed-rank (non-parametric) tests. We declared statistical significance when $p < 0.05$.

2.7. Results

Patient characteristics are detailed in Table 1. Patients included in this study predominantly exhibited HFrEF caused by non-ischemic (90%; $n = 8$) cardiomyopathy. However, 55% ($n = 5$) presented with coronary artery disease, and 44% presented with diabetes mellitus ($n = 4$). Echocardiography parameters are detailed in Table 2. All patients presented

with severely impaired systolic function as indicated by ejection fraction < 40%. Diastolic dysfunction, per recent recommendations [21] and clinical diagnosis, was also present in four patients but was not assessed in three patients due to severe systolic dysfunction.

Table 1. Patient characteristics.

	All Patients (n = 9)
Age (years)	55.9 ± 14.0
Male, % (n)	77.8 (7)
Ischemic CM, % (n)	11.1 (1)
Hypertension, % (n)	100 (9)
Hyperlipidemia, % (n)	55.6 (5)
Atrial fibrillation, % (n)	77.8 (7)
Asthma, % (n)	11.1 (1)
COPD, % (n)	22.2 (2)
CKD, % (n)	55.6 (5)
Diabetes mellitus, % (n)	44.4 (4)
CAD, % (n)	55.6 (5)

CM, cardiomyopathy; COPD, chronic obstructive pulmonary disease; CKD, chronic kidney disease; CAD, coronary artery disease.

Table 2. Echocardiography variables from patients included in the study.

	All Patients (n = 9)
EF (%)	17.2 ± 8.3
LVIDd (cm)	8.0 ± 1.2
LVIDs (cm)	7.3 ± 1.3
RVH (yes/no)	(4/5)
RVSP (mmHg)	42.4 ± 14.2
E wave (cm/s)	78.1 ± 25.6
A wave (cm/s)	61.4 ± 37.5
E' (cm/s)	8.19 ± 2.49
Dt (s)	155.2 ± 65.5
E/A	1.59 ± 0.78
E/E'	9.99 ± 3.21
E/DT (cm/s ²)	0.62 ± 0.38
Diastolic dysfunction Grade I/II/III (n, %)	1 (11)/2 (22)/1 (11)

EF, ejection fraction; LVIDd, left ventricular internal diameter during diastole; LVIDs, left ventricular internal diameter during systole; RVH, right ventricular hypertrophy determined by clinical assessment as 'yes' or 'no'; RVSP, right ventricular systolic pressure; DT, deceleration time. Diastolic function was considered normal in 2 patients and not assessed in 3 patients due to severe systolic dysfunction.

Treating isolated mitochondria with DTT improved the enzyme activities of complexes I and III by 230% ($p = 0.009$) and 86% ($p = 0.018$), respectively, while having no significant effect on complex II ($p = 0.630$) or IV ($p = 0.926$) activity (Figure 1). An overview of the creatine kinase clamp implemented to assess mitochondrial respiration, including a tracing of the rate of oxygen consumption and cellular conditions corresponding to different energetic states, is shown in Figure 2 and Table 3. Bundles treated with DTT displayed no significant differences in respiration under state 2 ($p = 0.588$) or the highest energetic demand tested (1 mM PCr) ($p = 0.312$) conditions (Figure 3A). There were no significant differences in OXPHOS conductance ($p = 0.439$) between control and DTT-treated bundles (Figure 3). Mitochondrial ADP kinetics also did not differ between groups for maximal oxygen consumption ($JO_{2\text{Max}}$) ($p = 0.287$) or ADP sensitivity (ADP_{50}) ($p = 0.514$) (Figure 4).

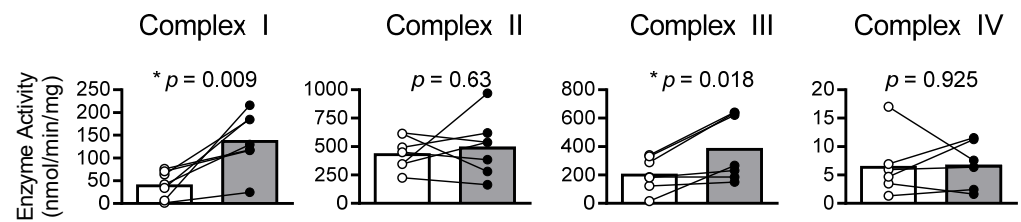


Figure 1. DTT treatment improves mitochondrial complex I and III enzyme activity. Enzyme activities of complexes of the electron transport system were assessed in isolated cardiomyocyte mitochondria from patients with HFrEF. The 5 mM DTT treatment (gray) improved activity of complexes I and III compared to controls (white) but had no effect on complex II or IV. Enzyme activities compared via paired *t*-test. * $p < 0.05$.

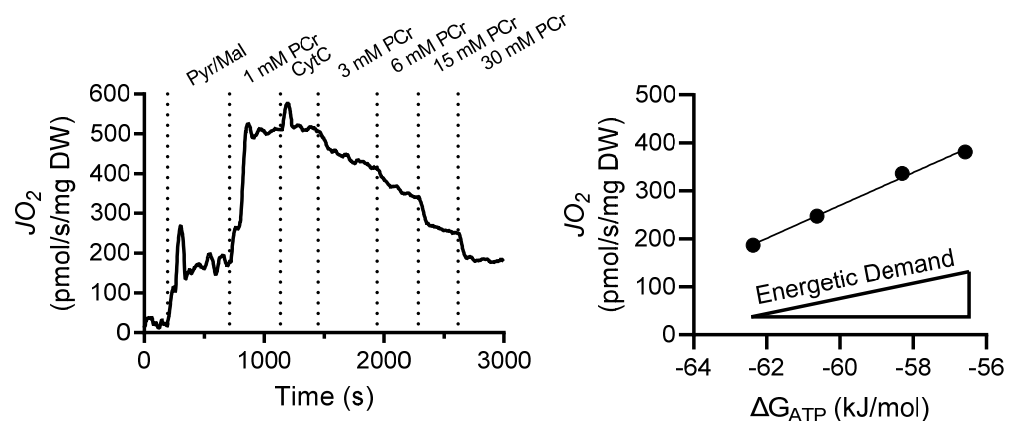


Figure 2. Creatine kinase clamp used to control mitochondrial energetic demand. Example tracing of the creatine kinase clamp in which PCr is titrated to control the mitochondrial energetic demand (ΔG_{ATP}) (see Table 3). ΔG_{ATP} is then plotted against oxygen consumption (J_{O_2}) in which the slope of the relationship represents the mitochondrial oxidative phosphorylation (OXPHOS) conductance.

Table 3. Bioenergetic conditions at each energetic state during the creatine kinase clamp assay.

PCr (mM)	ΔG_{ATP} (kJ/mol)	ADP (mM)	ATP (mM)	Cr (mM)
1	−54.16	0.176	4.82	4.824
3	−57.09	0.058	4.94	4.942
6	−58.32	0.037	4.96	4.963
15	−60.63	0.016	4.98	4.984
30	−62.37	0.009	4.99	4.991

Energetic conditions brought on by various titrations of PCr in the creatine kinase assay. Concentrations determined using the bioenergetics calculator provided by Fisher-Wellman et al. (2018) [18].

Diabetes worsens the metabolic and cardiac pathophysiologies in heart failure, resulting in exacerbated impairments in redox balance [22]. Thus, we compared the effects of DTT on mitochondrial function ($\Delta DTT = DTT - \text{untreated samples}$) between patients presenting with and without a diagnosis of diabetes mellitus. There were no significant differences in the effects of DTT between these patient groups (Supplementary Figure S1).

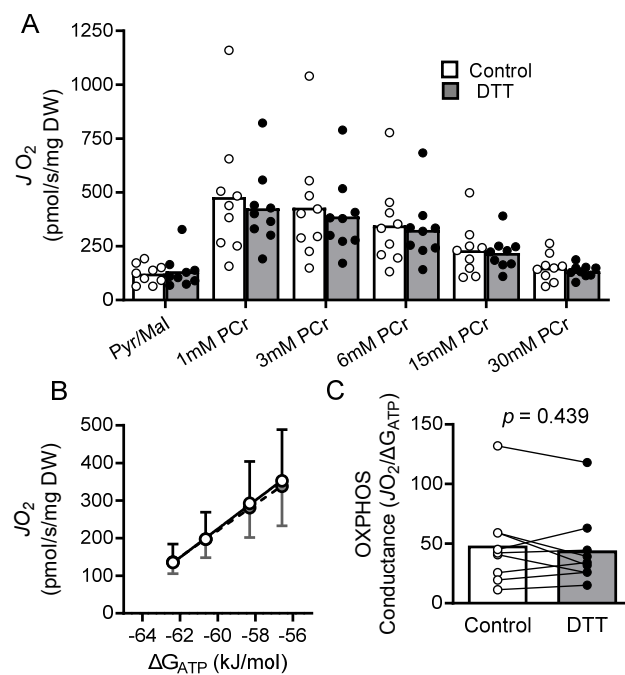


Figure 3. OXPHOS conductance does not improve with DTT treatment. Saponin-permeabilized cardiomyocyte bundles from patients with HFrEF did not experience improvements in mitochondrial respiration under various energetic states following treatment with 5 mM DTT (A). Energetic demand (ΔG_{ATP}) was manipulated through titrations of PCr (see Table 2) and plotted against the rate of oxygen consumption (J_{O_2}) (B) to determine OXPHOS conductance (C), which was also unaffected by DTT treatment. J_{O_2} and OXPHOS conductance of control and DTT-treated samples compared via paired *t*-test.

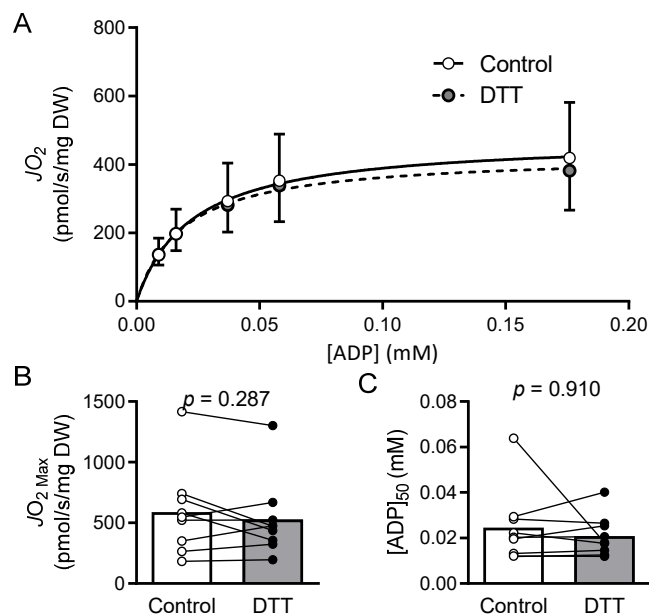


Figure 4. Mitochondrial ADP kinetics are unchanged by DTT treatment. (A) ADP concentrations corresponding to each energetic state were determined using the bioenergetics calculator from Fisher-Wellman et al. (2018) [18] (see Table 3) to determine Michaelis–Menten kinetics and the effects of 5 mM DTT treatment from respiration experiments presented in Figure 3. DTT treatment had no effect on maximal respiration ($J_{O_2_{Max}}$; compared via paired *t*-test) (B) or ADP sensitivity ($[ADP]_{50}$; compared via paired Wilcoxon signed-rank test) (C).

2.8. Discussion

The main findings of this study are that the thiol-reducing agent DTT acutely increased the activities of mitochondrial ETS complexes I and III but did not change complex III and IV activities, mitochondrial oxidative phosphorylation conductance, or the Michaelis–Menten kinetics of mitochondrial respiration in cardiomyocytes from patients with end-stage HFrEF. These findings suggest that reversible thiol oxidation, which impairs mitochondrial ETS complex activity, is not a limiting factor for mitochondrial metabolism and oxidative phosphorylation responses to carbohydrate-type substrates in the left ventricle of patients with end-stage heart failure.

2.9. Mitochondrial Bioenergetics and Dysfunction in HFrEF

The heart is considered the most metabolically active tissue in the body due to its continuous contractile activity. The lion's share of this energetic demand is met by mitochondria [23], which occupy ~30% of cell volume within cardiomyocytes [24]. Severe and end-stage HFrEF involves a myocardial energetic crisis in which sufficient energy cannot be produced to meet the workload of the heart [1–5]. There is a lower PCr/Cr ratio [7] and a lower total adenine pool [25], as well as a shift in substrate preference from free fatty acid oxidation to glycolysis. However, impairments in mitochondrial respiration are also evident under controlled substrate conditions. The mitochondrial and energetic deficiency correlates with patient mortality and has been posited as a primary driving force of HFrEF disease pathology [8].

With a greater recognition of the effect of mitochondrial dysfunction on overall disease pathology, these organelles have become increasingly popular targets for potential therapeutics for patients with HFrEF [8–10]. Mitochondrial-targeted therapeutics may be especially valuable for patients with end-stage HFrEF when conventional treatments (e.g., angiotensin-converting enzyme inhibitors and beta-blockers) are no longer effective. Investigations into myocardial mitochondrial function in ventricular biopsies from patients with end-stage HFrEF have revealed decreased mitochondrial respiration and decreased activity of individual complexes of the ETS [1–5]. In general, a specific dysfunction within the mitochondria has been attributed to complex I [1–3,26,27], complex II [2,5], complex III [28], complex IV [2,27,29], and several enzymes within the tricarboxylic acid cycle [1,2,27].

The ETS couples the movement of electrons down a redox potential gradient with the active transport of protons (H^+) against an electro-chemical gradient in order to generate a proton motive force that is then used to drive the formation of high-energy phosphates in the form of ATP. Complexes I and II initiate the movement of electrons into the ETS by oxidizing reducing equivalents, while complex IV facilitates the final transfer of electrons to O_2 to form H_2O . Complexes I, III, and IV couple electron flow with proton pumping, while complex V uses the established proton motive force to phosphorylate ADP and regenerate the molecules of ATP. The ratio of ATP/ADP is pushed far from equilibrium in favor of greater ATP by way of the proton motive force, and it is the displacement from equilibrium that establishes the free energy associated with ATP hydrolysis (ΔG_{ATP}) [30,31]. The flow of electrons through the ETS is limited by the development of the proton motive force, which, in turn, is limited by the equilibrium of ATP/ADP. As such, changes to ADP dictate the overall rate of mitochondrial respiration. ADP can change in response to an increased workload or, in the case of the creatine kinase assay, by manipulating the following reaction: $PCr + ADP \leftrightarrow Cr + ATP$. Traditional approaches used to measure mitochondrial function consist of measuring oxygen consumption under various energetic states that are induced by the addition of substrates, inhibitors, and high concentrations of ADP. While these experimental approaches have provided useful information about mitochondrial function, they disrupt the internal mitochondrial mechanisms of responding to energetic demand. Conversely, the mitochondrial creatine kinase clamp permits control over mitochondrial energetic demand by titrating different concentrations of PCr to monitor mitochondrial oxygen consumption at various physiologically relevant energetic states [18,32,33].

The creatine kinase clamp also provides several metrics that are similar to those presented with respiration experiments involving titrations of ADP up to saturating concentrations. State 2 refers to respiration in the presence of energizing substrates but in the absence of adenine molecules (ATP or ADP). Our values for state 2 respiration (Pyr/Mal) match those reported previously from patients with HFrEF when normalized by bundle wet weight (data not shown) [2]. Additionally, the energetic state elicited by 1 mM PCr represents a near-maximal energetic demand and is similar to the state 3 conditions elicited by maximal concentrations of ADP. The values of respiration at the highest level of energy demand within our conditions are similar to, or greater than, state III respiration presented in previous studies investigating myocardial mitochondrial function in patients with HFrEF [1,2,5]. These differences may be related to sample handling and preparation or experimental approach.

A traditional approach used to assess mitochondrial respiration involves the use of Michaelis–Menten kinetics to define ADP sensitivity (K_m ; ADP_{50}) and maximal capacity (V_{max}) [5,34]. We calculated ADP at each energetic state using the energetics calculator provided by Fisher-Wellman et al. [18] to determine the Michaelis–Menten ADP kinetics of mitochondrial respiration. The K_m of cardiac mitochondria has been reported as being 0.096 mM in healthy controls and 0.057 mM in patients with HFrEF [5]. These values reflect slightly lower ADP sensitivity than what we report here (0.025 mM in untreated samples), which likely results from differences in energetic conditions in the assay. Glutamate and malate were used as energizing substrates in the study cited above, while we used a combination of pyruvate and malate. Different substrate combinations can elicit differences in sensitivity and maximal respiration. Greater mitochondrial respiration in response to pyruvate over glutamate has been reported in murine hearts [18] and may carry over to sensitivity in humans. Additionally, when energetic states are controlled via titrations of PCr, maximal respiration is achieved at 0.176 mM of ADP, whereas traditional ADP titration experiments that disrupt the extramitochondrial energetic control expose mitochondria to upwards of 4 mM ADP. Acknowledging experimental bioenergetic conditions is important to compare these results across studies. We also report JO_2_{Max} calculated from Michaelis–Menten ADP kinetics, which is essentially equivalent to JO_2 at 1 mM PCr discussed above.

2.10. Myocardial Oxidized Shifts

A key feature of and a contributing factor to myocardial dysfunction in HFrEF is the excessive accumulation of reactive oxygen species (ROS). Markers of an oxidized shift in the cellular redox tone have been observed in ventricular biopsies from patients with HFrEF [14,27,35]. The mitochondria are a prominent source of increased ROS production and, by proximity, a target of redox reactions. While there are reports of decreased mitochondrial content that contribute to energetic insufficiency [5], Sheeran et al. [27] argue that mitochondrial dysfunction stems from oxidized post-translational modifications that impair enzyme and organelle functions. They report increased markers of oxidation on the subunits of complexes I, IV, and V of the ETS that correspond to decreased enzyme activity [27], while redox proteomics in ventricular biopsies also observed the increased oxidation of subunits associated with complexes I and II [14]. Specifically, five subunits in complex I showed increased markers of oxidation (carbonylation and nitrotyrosine), and all subunits contain Fe-S clusters that facilitate the transfer of electrons. Similarly, subunits I and II of complex IV contain redox centers that are directly involved in the transfer of electrons from Cytochrome C to O_2 [27]. These oxidative post-translational modifications have been suggested to be contributors to mitochondrial enzymatic function and may be an important target to improve mitochondrial function and the energetic crisis in HFrEF [9,27].

Several processes within the mitochondria are regulated by redox switches, which have recently been reviewed [12,13]. Specifically, several studies have investigated the role of thiol oxidation on mitochondrial function, predominately investigating the role of the glutathionylation of cysteine residues [36–38]. Cysteines are commonly observed near active sites of enzymes because of their ability to stabilize Fe-S clusters. Two cysteines on

the 75 kDa subunit of complex I (NDUSFI) (Cys⁵³¹ and Cys⁷⁰⁴) are particularly sensitive to redox reactions that can impair enzyme function [39–41]. While specific cysteines were not investigated in the current study, the NDUSFI subunit experienced significant oxidative shifts in myocardial biopsies from patients with HFrEF compared to controls in a previous study [14]. It follows that redox reactions on these residues may relate to impaired function that can be targeted with a reducing agent.

Dithiothreitol (DTT), also known as Cleland's reagent, is a molecular compound characterized as a potent reducing agent in 1964 [42]. With its low redox potential (−0.33 V at pH 7), DTT is frequently used in molecular and biochemical experiments to directly reduce reversible oxidized disulfide bonds that form on cysteine. Acute DTT exposure *in vitro* has been found to effectively improve enzyme activity following an oxidized shift in the cellular redox tone under several conditions. Improvements in striated muscle with DTT exposure include proteins involved in contractile [43] and mitochondrial functions [15,16,44,45]. Mice on a high-fat, high-sucrose diet have decreased cardiac mitochondrial function due to impaired complex II activity that is attenuated with *in vitro* DTT treatment [15]. DTT treatment has also been found to improve mitochondrial dysfunction associated with drug toxicity in rats [16,46]. It is important to acknowledge that the direct exposure of isolated mitochondria to the thiol-oxidizing agent diamide impaired complex I and III activity, and this was not attenuated with DTT treatment [39]. This may be due to different outcomes from reversible endogenous vs. irreversible exogenous oxidant exposure, or possibly through oxidant effects on the recruitment of binding partners that augment enzyme function [39].

Our study shows that reversible thiol oxidation also modulates mitochondrial ETS complex activity in the human heart. Specifically, our data provide evidence that DTT heightened the enzymatic activities of complexes I and III in mitochondria isolated from the left ventricle of patients with end-stage heart failure. However, this increase in ETS complex activity did not translate into higher measures of mitochondrial respiration in permeabilized cardiomyocytes. The discrepant effect of DTT on the activity of ETS complex measures of respiration may be explained by several factors. First, enzyme activity assays were conducted in the presence of DTT, while respiration experiments consisted of a pre-treatment before measurements in the absence of DTT. It is possible that thiol residues that were reduced during the DTT treatment during the wash stage were re-oxidized when cardiomyocytes were placed into the respiration buffer, as cardiac mitochondrial ROS is increased in end-stage HFrEF. Second, protein thiols may have been more accessible for DTT in isolated mitochondria than in permeabilized bundles. Third, improved enzyme activity via the reduction of oxidized thiol groups in complexes I and III may only be detectable when the enzyme activity is not constrained by the mitochondrial membrane potential. As described above, the flow of electrons through the ETS in an *in-tact* system is limited at distinct control nodes, including the establishment of the membrane potential [18,31]. The maximal activity of individual complexes may exceed that permitted by the thermodynamic constraints of the complete system. Fourth, cardiac mitochondria complex I and III activities may not be rate limiting for respiration in patients with end-stage HFrEF. Other steps of mitochondrial energy transfer could limit respiration and oxidative phosphorylation conductance (e.g., matrix dehydrogenases, complex IV, and complex V/ATP synthesis). Our experiments found no improvement in complex IV function with DTT. Additionally, the cardiomyocytes of patients with end-stage HFrEF have a lower abundance of CoQ10; this facilitates the transfer of electrons from complexes I and II to complex III, which contributes to mitochondrial dysfunction [47]. We did not measure the effects of DTT on the activity of matrix dehydrogenases or complex V, as these assays were not justified by our results showing that DTT had no effect on oxidative phosphorylation conductance.

2.11. Limitations

We did not have access to ventricular biopsies from control subjects to compare mitochondrial oxidative phosphorylation conductance and ETS complex activities from patients with HFrEF and to compare the potential role of DTT. However, several previous studies

have established decreased mitochondrial respiration in HFrEF using ventricular biopsies from patients with HFrEF compared to healthy donor hearts [1,2]. In healthy rodent hearts, DTT treatment has been found to have no effect [15] or has been found to decrease [16] myocardial mitochondrial function, suggesting that any effects of DTT in our study would arise from reversing the oxidized thiol shift seen with end-stage HFrEF [27]. Our preparation focused on ETS complex activities, mitochondrial energy transfer conductance, and respiration under controlled conditions in the presence of glycolytic substrates. The shift in cardiac mitochondrial substrate in HFrEF is largely attributed to the activation of a fetal gene program that favors glycolytic over fatty acid metabolism [11], but matrix dehydrogenases associated with fatty acid oxidation may also undergo thiol oxidation, which diminishes enzyme activity and contributes to the cardiac energy substrate shift in HFrEF. The substrate shift may be a protective compensatory response to an energy transfer system that is less ROS sensitive, as our study suggests as being the case for pyruvate metabolism by cardiac mitochondria. We did not determine which amino acid residues were affected by treatment with DTT, but it is reasonable to expect that all accessible residues would have been reduced with our protocol. Importantly, our goal was to examine the general impact of thiol oxidation on mitochondrial bioenergetics with the primary energy source in end-stage HFrEF. It is also not possible to distinguish the impact of other oxidative modifications, which are not acutely reversed by DTT, on mitochondrial function. These would require chronic treatment with antioxidants *in vivo*. Some of the discrepant findings in oxidative phosphorylation conductance and respiration vs. ETS complex enzyme activity could arise from the use of fresh vs. frozen samples, respectively. We could not perform ETS enzyme activity assays in fresh samples due to technical challenges. Finally, we did not have enough subjects to differentiate between effects in patients with ischemic and non-ischemic HFrEF. Mitochondrial dysfunction has been observed in both patient populations but is reportedly worse in ischemic HFrEF [2]. We also attempted to differentiate the effect of DTT between patients with and without diabetes mellitus. Although we had a limited sample size to define the impact of diabetes on the outcomes of our study, the data suggest similar effects of DTT in diabetic and non-diabetic individuals with heart failure. Given the size and heterogeneity of our population, which reflects the realities of clinical settings, our findings of improved complex activity appear even more robust.

3. Conclusions

Cardiac and mitochondrial redox imbalances are common features of HFrEF that contribute to dysfunction. Our study indicates that treatment with DTT, a potent reducing agent, can increase the enzyme activity of complexes I and III of the ETS in mitochondria isolated from HFrEF ventricular biopsies. These effects did not translate to greater mitochondrial respiration measured in permeabilized cardiomyocyte bundles, suggesting that other components of mitochondrial energy transfer are rate limiting for respiration and, presumably, ATP synthesis in end-stage HFrEF. However, our data indicate that human cardiac mitochondrial respiratory function can be modulated through reversible thiol oxidation. Therefore, optimal therapies to normalize cardiac mitochondrial respiration in patients with end-stage HFrEF will likely require interventions to reverse thiol oxidation, which limits complex I and III activities in this population.

Supplementary Materials: The following supporting information can be downloaded at: <https://www.mdpi.com/article/10.3390/cells11152292/s1>. Figure S1. Comparisons between patients with and without diabetes mellitus. Δ DTT (DTT—un-treated samples) for mitochondrial parameters assessed in isolated mitochondria (A); and permeabilized cardiomyocyte bundles (B–D). There were no observable differences for the effects of DTT between patients with and without diabetes for (A) mitochondrial ETS enzyme activities, (B) OXPHOS Conductance, (C) maximal respiration, or (D) ADP sensitivity. Groups compared made via independent *t*-test.

Author Contributions: Conceptualization, R.A.K., T.E.R., E.I.J. and L.F.F.; methodology, R.A.K., T.T., T.E.R. and L.F.F.; formal analysis, R.A.K., O.M.S., T.E.R. and L.F.F.; data curation, R.A.K., O.M.S., G.J.A. and E.I.J.; writing—original draft preparation, R.A.K.; writing—review and editing, R.A.K., T.T., O.M.S., T.E.R., G.J.A., E.I.J. and L.F.F.; funding acquisition, E.I.J. and L.F.F. All authors have read and agreed to the published version of the manuscript.

Funding: The study was funded by the University of Florida (P0175597-DRPD-ROF2020).

Institutional Review Board Statement: The study was conducted in accordance with the Declaration of Helsinki, and approved by the Institutional Review Board of the University of Florida (protocol #202000853, approved 15/09/2021).

Informed Consent Statement: Informed consent was obtained from all subjects involved in the study (protocol #202000853, approved 15/09/2021).

Data Availability Statement: The data that support the findings in this study are available from the corresponding author upon reasonable request.

Acknowledgments: R. Kumar received a predoctoral fellowship from the American Heart Association (20PRE35200047). L. Ferreira was supported by NIH R01 HL1331806 and the University of Florida Research Foundation Professorship. T. Ryan was funded by NIH R01 HL149704. E. Jeng was supported by NIH R01 NR020175.

Conflicts of Interest: The authors have no conflicts of interest. G.A. was a consultant for Terumo Aortic Ltd. on activities unrelated to the current study.

References

1. Lemieux, H.; Semsroth, S.; Antretter, H.; Höfer, D.; Gnaiger, E. Mitochondrial respiratory control and early defects of oxidative phosphorylation in the failing human heart. *Int. J. Biochem. Cell Biol.* **2011**, *43*, 1729–1738. [[CrossRef](#)] [[PubMed](#)]
2. Park, S.Y.; Trinity, J.D.; Gifford, J.R.; Diakos, N.A.; McCreath, L.; Drakos, S.; Richardson, R.S. Mitochondrial function in heart failure: The impact of ischemic and non-ischemic etiology. *Int. J. Cardiol.* **2016**, *220*, 711–717. [[CrossRef](#)] [[PubMed](#)]
3. Schipper, D.A.; Palsma, R.; Marsh, K.M.; O'Hare, C.; Dicken, D.S.; Lick, S.; Kazui, T.; Johnson, K.; Smolenski, R.T.; Duncker, D.J.; et al. Chronic Myocardial Ischemia Leads to Loss of Maximal Oxygen Consumption and Complex I Dysfunction. *Ann. Thorac. Surg.* **2017**, *104*, 1298–1304. [[CrossRef](#)] [[PubMed](#)]
4. Sharov, V.G.; Todor, A.V.; Silverman, N.; Goldstein, S.; Sabbah, H.N. Abnormal mitochondrial respiration in failed human myocardium. *J. Mol. Cell. Cardiol.* **2000**, *32*, 2361–2367. [[CrossRef](#)] [[PubMed](#)]
5. Stride, N.; Larsen, S.; Hey-Mogensen, M.; Sander, K.; Lund, J.T.; Gustafsson, F.; Køber, L.; Dela, F. Decreased mitochondrial oxidative phosphorylation capacity in the human heart with left ventricular systolic dysfunction. *Eur. J. Heart Fail.* **2013**, *15*, 150–157. [[CrossRef](#)] [[PubMed](#)]
6. Neubauer, S.; Horn, M.; Pabst, T.; Gödde, M.; Lübke, D.; Jilling, B.; Hahn, D.; Ertl, G. Contributions of 31P-magnetic resonance spectroscopy to the understanding of dilated heart muscle disease. *Eur. Heart J.* **1995**, *16* (Suppl. O), 115–118. [[CrossRef](#)] [[PubMed](#)]
7. Neubauer, S.; Horn, M.; Cramer, M.; Harre, K.; Newell, J.B.; Peters, W.; Pabst, T.; Ertl, G.; Hahn, D.; Ingwall, J.S.; et al. Myocardial Phosphocreatine-to-ATP Ratio Is a Predictor of Mortality in Patients With Dilated Cardiomyopathy. *Circulation* **1997**, *96*, 2190–2196. [[CrossRef](#)]
8. Neubauer, S. The failing heart—an engine out of fuel. *N. Engl. J. Med.* **2007**, *356*, 1140–1151. [[CrossRef](#)]
9. Kiyuna, L.A.; Albuquerque, R.P.E.; Chen, C.H.; Mochly-Rosen, D.; Ferreira, J.C.B. Targeting mitochondrial dysfunction and oxidative stress in heart failure: Challenges and opportunities. *Free Radic. Biol. Med.* **2018**, *129*, 155–168. [[CrossRef](#)]
10. Brown, D.A.; Perry, J.B.; Allen, M.E.; Sabbah, H.N.; Stauffer, B.L.; Shaikh, S.R.; Cleland, J.G.; Colucci, W.S.; Butler, J.; Voors, A.A.; et al. Expert consensus document: Mitochondrial function as a therapeutic target in heart failure. *Nat. Rev. Cardiol.* **2017**, *14*, 238–250. [[CrossRef](#)]
11. Stanley, W.C.; Recchia, F.A.; Lopaschuk, G.D. Myocardial substrate metabolism in the normal and failing heart. *Physiol. Rev.* **2005**, *85*, 1093–1129. [[CrossRef](#)] [[PubMed](#)]
12. Nietzel, T.; Mostertz, J.; Hochgräfe, F.; Schwarzländer, M. Redox regulation of mitochondrial proteins and proteomes by cysteine thiol switches. *Mitochondrion* **2017**, *33*, 72–83. [[CrossRef](#)] [[PubMed](#)]
13. Mailloux, R.J.; Jin, X.; Willmore, W.G. Redox regulation of mitochondrial function with emphasis on cysteine oxidation reactions. *Redox Biol.* **2013**, *2*, 123–139. [[CrossRef](#)] [[PubMed](#)]
14. Tomin, T.; Schittmayer, M.; Sedej, S.; Bugger, H.; Gollmer, J.; Honeder, S.; Darnhofer, B.; Liesinger, L.; Zuckermann, A.; Rainer, P.P.; et al. Mass Spectrometry-Based Redox and Protein Profiling of Failing Human Hearts. *Int. J. Mol. Sci.* **2021**, *22*, 1787. [[CrossRef](#)]
15. Sverdlov, A.L.; Elezaby, A.; Behring, J.B.; Bachschmid, M.M.; Luptak, I.; Tu, V.H.; Siwik, D.A.; Miller, E.J.; Liesa, M.; Shirihai, O.S.; et al. High fat, high sucrose diet causes cardiac mitochondrial dysfunction due in part to oxidative post-translational modification of mitochondrial complex II. *J. Mol. Cell. Cardiol.* **2015**, *78*, 165–173. [[CrossRef](#)]

16. Oliveira, P.J.; Santos, M.S.; Wallace, K.B. Doxorubicin-induced thiol-dependent alteration of cardiac mitochondrial permeability transition and respiration. *Biochemistry* **2006**, *71*, 194–199. [[CrossRef](#)]
17. Thome, T.; Kumar, R.A.; Burke, S.K.; Khattri, R.B.; Salyers, Z.R.; Kelley, R.C.; Coleman, M.D.; Christou, D.D.; Hepple, R.T.; Scali, S.T.; et al. Impaired muscle mitochondrial energetics is associated with uremic metabolite accumulation in chronic kidney disease. *JCI Insight*. **2020**, *6*, e139826. [[CrossRef](#)]
18. Fisher-Wellman, K.H.; Davidson, M.T.; Narowski, T.M.; Lin, C.T.; Koves, T.R.; Muoio, D.M. Mitochondrial Diagnostics: A Multiplexed Assay Platform for Comprehensive Assessment of Mitochondrial Energy Fluxes. *Cell Rep*. **2018**, *24*, 3593–3606.e10. [[CrossRef](#)]
19. Thome, T.; Salyers, Z.R.; Kumar, R.A.; Hahn, D.; Berru, F.N.; Ferreira, L.F.; Scali, S.T.; Ryan, T.E. Uremic metabolites impair skeletal muscle mitochondrial energetics through disruption of the electron transport system and matrix dehydrogenase activity. *Am. J. Physiol. Cell Physiol*. **2019**, *317*, C701–C713. [[CrossRef](#)]
20. Spinazzi, M.; Casarin, A.; Pertegato, V.; Salviati, L.; Angelini, C. Assessment of mitochondrial respiratory chain enzymatic activities on tissues and cultured cells. *Nat. Protoc*. **2012**, *7*, 1235–1246. [[CrossRef](#)]
21. Mitter, S.S.; Shah, S.J.; Thomas, J.D. A Test in Context: E/A and E/e' to Assess Diastolic Dysfunction and LV Filling Pressure. *J. Am. Coll. Cardiol*. **2017**, *69*, 1451–1464. [[CrossRef](#)] [[PubMed](#)]
22. Dunlay, S.M.; Givertz, M.M.; Aguilar, D.; Allen, L.A.; Chan, M.; Desai, A.S.; Deswal, A.; Dickson, V.V.; Kosiborod, M.N.; Lekavich, C.L.; et al. Type 2 Diabetes Mellitus and Heart Failure: A Scientific Statement From the American Heart Association and the Heart Failure Society of America: This statement does not represent an update of the 2017 ACC/AHA/HFSA heart failure guideline update. *Circulation* **2019**, *140*, e294–e324. [[CrossRef](#)] [[PubMed](#)]
23. Opie, L.H. *Heart Physiology: From Cell to Circulation*; Lippincott Williams & Wilkins: Philadelphia, PA, USA, 2004.
24. Barth, E.; Stämmler, G.; Speiser, B.; Schaper, J. Ultrastructural quantitation of mitochondria and myofilaments in cardiac muscle from 10 different animal species including man. *J. Mol. Cell. Cardiol*. **1992**, *24*, 669–681. [[CrossRef](#)]
25. Wu, F.; Zhang, J.; Beard, D.A. Experimentally observed phenomena on cardiac energetics in heart failure emerge from simulations of cardiac metabolism. *Proc. Natl. Acad. Sci. USA* **2009**, *106*, 7143–7148. [[CrossRef](#)] [[PubMed](#)]
26. Scheubel, R.J.; Tostlebe, M.; Simm, A.; Rohrbach, S.; Prondzinsky, R.; Gellerich, F.N.; Silber, R.-E.; Holtz, J. Dysfunction of mitochondrial respiratory chain complex I in human failing myocardium is not due to disturbed mitochondrial gene expression. *J. Am. Coll. Cardiol*. **2002**, *40*, 2174–2181. [[CrossRef](#)]
27. Sheeran, F.L.; Pepe, S. Posttranslational modifications and dysfunction of mitochondrial enzymes in human heart failure. *Am. J. Physiol. Endocrinol. Metab*. **2016**, *311*, E449–E460. [[CrossRef](#)]
28. Jarreta, D.; Orus, J.; Barrientos, A.; Miro, O.; Roig, E.; Heras, M.; Moraes, C.T.; Cardellach, F.; Casademont, J. Mitochondrial function in heart muscle from patients with idiopathic dilated cardiomyopathy. *Cardiovasc. Res*. **2000**, *45*, 860–865. [[CrossRef](#)]
29. Chaanine, A.H.; Joyce, L.D.; Stulak, J.M.; Maltais, S.; Joyce, D.L.; Dearani, J.A.; Klaus, K.; Nair, K.S.; Hajjar, R.J.; Redfield, M.M. Mitochondrial Morphology, Dynamics, and Function in Human Pressure Overload or Ischemic Heart Disease with Preserved or Reduced Ejection Fraction. *Circ. Heart Fail*. **2019**, *12*, e005131. [[CrossRef](#)]
30. Neuffer, P.D. The Bioenergetics of Exercise. *Cold Spring Harb. Perspect. Med*. **2018**, *8*, a029678. [[CrossRef](#)]
31. Nicholls, D.G.; Ferguson, S. *Bioenergetics*, 4th ed.; Elsevier: Amsterdam, The Netherlands, 2013; pp. 1–419.
32. Willis, W.T.; Jackman, M.R.; Messer, J.I.; Kuzmiak-Glancy, S.; Glancy, B. A Simple Hydraulic Analog Model of Oxidative Phosphorylation. *Med. Sci. Sports Exerc*. **2016**, *48*, 990–1000. [[CrossRef](#)]
33. Glancy, B.; Willis, W.T.; Chess, D.J.; Balaban, R.S. Effect of calcium on the oxidative phosphorylation cascade in skeletal muscle mitochondria. *Biochemistry* **2013**, *52*, 2793–2809. [[CrossRef](#)] [[PubMed](#)]
34. Saks, V.A.; Belikova, Y.O.; Kuznetsov, A.V.; Khuchua, Z.A.; Branishte, T.H.; Semenovskiy, M.L.; Naumov, V.G. Phosphocreatine pathway for energy transport: ADP diffusion and cardiomyopathy. *Am. J. Physiol.-Heart Circ. Physiol*. **1991**, *261*, 30–38. [[CrossRef](#)]
35. Sheeran, F.L.; Rydström, J.; Shakhparonov, M.I.; Pestov, N.B.; Pepe, S. Diminished NADPH transhydrogenase activity and mitochondrial redox regulation in human failing myocardium. *Biochim. Biophys. Acta* **2010**, *1797*, 1138–1148. [[CrossRef](#)] [[PubMed](#)]
36. Mailloux, R.J.; Xuan, J.Y.; Beauchamp, B.; Jui, L.; Lou, M.; Harper, M.E. Glutaredoxin-2 is required to control proton leak through uncoupling protein-3. *J. Biol. Chem*. **2013**, *288*, 8365–8379. [[CrossRef](#)] [[PubMed](#)]
37. Wu, H.; Lin, L.; Giblin, F.; Ho, Y.S.; Lou, M.F. Glutaredoxin 2 knockout increases sensitivity to oxidative stress in mouse lens epithelial cells. *Free Radic. Biol. Med*. **2011**, *51*, 2108–2117. [[CrossRef](#)]
38. Hill, B.G.; Higdon, A.N.; Dranka, B.P.; Darley-Usmar, V.M. Regulation of vascular smooth muscle cell bioenergetic function by protein glutathiolation. *Biochim. Biophys. Acta* **2010**, *1797*, 285–295. [[CrossRef](#)]
39. Hurd, T.R.; Requejo, R.; Filipovska, A.; Brown, S.; Prime, T.A.; Robinson, A.J.; Fearnley, I.M.; Murphy, M.P. Complex I within oxidatively stressed bovine heart mitochondria is glutathionylated on Cys-531 and Cys-704 of the 75-kDa subunit: Potential role of CYS residues in decreasing oxidative damage. *J. Biol. Chem*. **2008**, *283*, 24801–24815. [[CrossRef](#)]
40. Beer, S.M.; Taylor, E.R.; Brown, S.E.; Dahm, C.C.; Costa, N.J.; Runswick, M.J.; Murphy, M.P. Glutaredoxin 2 catalyzes the reversible oxidation and glutathionylation of mitochondrial membrane thiol proteins: Implications for mitochondrial redox regulation and antioxidant DEFENSE. *J. Biol. Chem*. **2004**, *279*, 47939–47951. [[CrossRef](#)]
41. Taylor, E.R.; Hurrell, F.; Shannon, R.J.; Lin, T.K.; Hirst, J.; Murphy, M.P. Reversible glutathionylation of complex I increases mitochondrial superoxide formation. *J. Biol. Chem*. **2003**, *278*, 19603–19610. [[CrossRef](#)]
42. Cleland, W.W. Dithiothreitol, a New Protective Reagent for SH Groups*. *Biochemistry* **1964**, *3*, 480–482. [[CrossRef](#)]

43. Andrade, F.H.; Reid, M.B.; Allen, D.G.; Westerblad, H. Effect of hydrogen peroxide and dithiothreitol on contractile function of single skeletal muscle fibres from the mouse. *J. Physiol.* **1998**, *509*, 565–575. [[CrossRef](#)] [[PubMed](#)]
44. Wang, S.B.; Foster, D.B.; Rucker, J.; O'Rourke, B.; Kass, D.A.; Van Eyk, J.E. Redox regulation of mitochondrial ATP synthase: Implications for cardiac resynchronization therapy. *Circ. Res.* **2011**, *109*, 750–757. [[CrossRef](#)] [[PubMed](#)]
45. Borutaite, V.; Budriunaite, A.; Brown, G.C. Reversal of nitric oxide-, peroxynitrite- and S-nitrosothiol-induced inhibition of mitochondrial respiration or complex I activity by light and thiols. *Biochim. Biophys. Acta (BBA)-Bioenerg.* **2000**, *1459*, 405–412. [[CrossRef](#)]
46. Omidi, M.; Niknahad, H.; Mohammadi-Bardbori, A. Dithiothreitol (DTT) rescues mitochondria from nitrofurantoin-induced mitotoxicity in rat. *J. Biochem. Mol. Toxicol.* **2016**, *30*, 588–592. [[CrossRef](#)]
47. Sharma, A.; Fonarow, G.C.; Butler, J.; Ezekowitz, J.A.; Felker, G.M. Coenzyme Q10 and Heart Failure: A State-of-the-Art Review. *Circ. Heart Fail.* **2016**, *9*, e002639. [[CrossRef](#)]